Solid State Phenomena
ISSN: 1662-9779, Vol. 389, pp 181-189
doi:10.4028/p-f59c2L

Submitted: 2026-01-19
Accepted: 2026-02-16
Online: 2026-04-16

Mitigation of Geometric Inaccuracy in Closed-Contour Incremental Sheet Forming via Curvilinear Toolpath

Zixuan Mu[1,a*], Youngrok Lee[1,b], Jeffrey Abell[1,c], Alan Taub[1,2,d], Mihaela Banu[1,e]

[1]Department of Mechanical Engineering, University of Michigan, 2350 Hayward St, Ann Arbor, MI, USA

[2]Department of Materials Science and Engineering, University of Michigan, 2300 Hayward St, Ann Arbor, MI, USA

[a]zixuanmu@umich.edu, [b]yroklee@umich.edu, [c]jaabell@umich.edu, [d]alantaub@umich.edu, [e]mbanu@umich.edu

Keywords: incremental sheet forming (ISF), toolpath strategies, curvilinear, springback, bulge, pillow effect, bending moments

Abstract. Geometric deviations remain a major barrier to the widespread industrial adoption of incremental sheet forming (ISF). Compared with conventional toolpath compensation that rely on extensive data generation and trial-and-error procedures, variation of toolpath styles offers a more direct and efficient strategy for mitigating geometric defects. In this study, multiple curvilinear toolpath strategies were investigated for a standard closed-contour ISF part to evaluate their effectiveness in reducing geometric deviations. Six toolpaths were examined, including three established types – convex, concave, and wavy – and three novel toolpaths proposed in this work: adaptive, cusp, and sine. The convex toolpath achieved the largest side-wall springback reduction relative to the linear baseline but introduced a significant bottom pillow effect and reduced formability. While the cusp toolpath effectively suppressed both springback and pillow formation, it resulted in local thickening and degraded surface finish. Overall, the sine toolpath provided the most balanced performance, achieving effective reduction of all major geometric defects. Numerical simulations reveal an inherent tradeoff between side-wall springback reduction and bottom pillow formation, as positive residual bending moments formed in the pillow region contribute to springback mitigation by promoting outward bending of the side walls.

Introduction

Incremental sheet forming (ISF) has been extensively investigated over the past two decades and has demonstrated significant potential for small-batch manufacturing and rapid prototyping. Nevertheless, its relatively low geometric accuracy remains a major limitation that restricts broader industrial adoption. Such inaccuracies are commonly referred to sheet bending, springback, and pillow effect [1, 2]. Multiple approaches have been proposed to tackle this challenge [1], with toolpath compensation being the most commonly adopted strategy.

On one hand, geometric inaccuracies can arise from machine compliance effects, such as tool deflection, which are particularly significant in two-point incremental forming (TPIF) and robotic incremental forming [3, 4]. These compliance-induced errors can be systematically mitigated using compliance-based compensation strategies without extensive trial-and-error [3]. On the other hand, additional geometric inaccuracies stem from variations in the sheet stress mechanics during forming, which are often feature-dependent and difficult to compensate uniformly. This has motivated the development of predictive models for geometric deviation estimation. For instance, regression-based [5], simulation-assisted in-situ [6], and deep learning-based [7] approaches have been proposed to enable toolpath correction. While these studies have demonstrated significant success in reducing geometric deviations, most existing toolpath compensation strategies rely on extensive trial-and-error procedures or data-driven approaches that require large amounts of training data, which can be prohibitively expensive for sophisticated models.

As an alternative to explicit toolpath compensation, recent studies have increasingly focused on the design of toolpath strategies in ISF to influence stress evolution and deformation mechanisms during forming, thereby inherently improving geometric accuracy without iterative correction. While contour (Z-level) and spiral toolpaths remain the most conventional approaches, Lu et al. [8] developed a feature-based toolpath generation algorithm and demonstrated improved geometric accuracy for critical edges and non-symmetric parts. Other studies have explored alternative strategies, including muti-step [9, 10], zigzag [11], radial [12], point contact [13] toolpaths. Among these approaches, curvilinear toolpath strategies have attracted particular attention for their potential to influence the deformation behavior.

The concept of curvilinear toolpaths was first introduced by Grimm et al. [14], inspired by vibration-assisted forming, who showed that wavy toolpaths could improve surface variability. Building on this idea, Bremen and Bailly [15] investigated global springback by proposing convex and concave curvilinear toolpaths with superimposed wavy patterns. They showed that the wavy convex toolpath led to the minimum springback, as it effectively hindered the accumulation of local bending moments along the toolpath, resulting in a much smaller net residual bending moment prior to unclamping. However, their investigation was limited to open-contour parts clamped along two edges, which are more susceptible to large springback. In contrast, closed-contour parts, although generally stiffer and less prone to geometric inaccuracies, are more commonly used in ISF and exhibit distinct internal deformation mechanisms. The influence of curvilinear toolpaths on geometric deviations in closed-contour parts therefore remains insufficiently elaborated.

Consequently, this work follows a framework similar to that of Bremen and Bailly [15] and aims to examine the effects of different curvilinear toolpath strategies on the geometric deviation of a standard closed-contour ISF part, with the objective of identifying an effective strategy for reducing various geometric deviations and clarifying the underlying deformation mechanisms.

Methods

In this work, aluminum alloy 7075-O (Kaiser Aluminum, USA) was used to form all parts, and its tensile behavior was characterized using the Voce hardening law, as given in Eq. 1, with the corresponding parameters listed in Table 1 [16], where $\bar{\sigma}$ is the equivalent stress and ε^p is the equivalent plastic strain.

$$\bar{\sigma} = k_0 + Q(1 - e^{-\beta\varepsilon^p}) \quad (1)$$

Table 1. Elastic properties and Voce law parameters of AA7075-O

Density [kg/m^3]	Modulus [GPa]	Poisson's ratio	Yield strength [MPa]	k_0 [MPa]	Q [MPa]	β
2810	69.74	0.33	89	91.30	149.34	26.71

The truncated pyramid was chosen as the standard closed-contour target geometry in this study, with its dimensions and a representative formed part shown in Fig. 1 (a) and (b). Single point incremental forming (SPIF) experiments were performed on a 3-axis HAAS VF-2 CNC milling machine (Haas Automation, USA) using a 12.7 mm diameter hemispherical forming tool, as illustrated in Fig. 1 (c). The lubrication grease molybdenum disulfide (MoS_2) was applied prior to forming to reduce friction. All tests with different toolpaths were conducted at a feed rate of 42 mm/s and a step size of 0.5 mm. The formed geometries were measured using a Romer Absolute Arm with Integrated Scanner 7525SI (Hexagon Manufacturing Intelligence, USA).

Finite element simulations were performed using ABAQUS/Explicit. The forming tool and clamping frames were modeled as rigid bodies, while the sheet was discretized using 3D reduced-integration solid elements (C3D8R). A mesh size of 0.5 mm × 0.5 mm was adopted in the forming region, which has been shown to be appropriate based on a mesh sensitivity study in previous work

[16]. Five elements were used through the sheet thickness. The material behavior was modeled using the von Mises yield criterion with isotropic hardening.

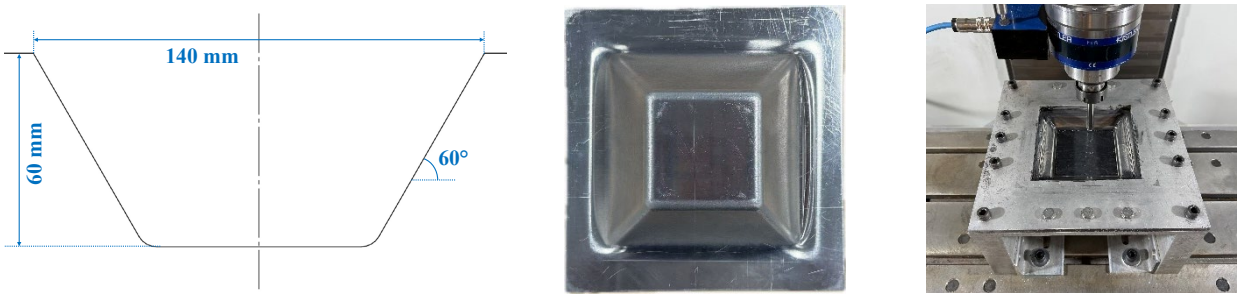

Fig. 1. Target geometry and experimental configuration: (a) CAD definition and dimensions of the truncated pyramid, (b) formed pyramidal part, and (c) ISF test setup.

Owing to the high rigidity of the target geometry, local springback following tool passage dominates over global springback during unclamping and trimming, leading to negligible differences in geometry before and after unclamping. Accordingly, all geometric defects considered in this study are treated as developing progressively during the forming process rather than occurring abruptly after forming. Since the magnitude of springback is directly governed by bending moments [17], and bending moment is not available as a direct field output for solid elements, bending moments, were therefore computed in the simulation using the simplified expression given in Eq. 2,

$$\mathbf{SM} = \int_{-t/2}^{t/2} \boldsymbol{\sigma}\, z\, dz \approx \sum_{e=1}^{N} \boldsymbol{\sigma}_e\, z_e\, \Delta z_e \tag{2}$$

where **SM** is the section bending moment, $\boldsymbol{\sigma}$ is the normal stress, z is the through-thickness coordinate measured from the mid-plane, t is the deformed sheet thickness, e denotes the through-thickness element index, N is the number of elements through the thickness, and Δz refers to deformed element thickness.

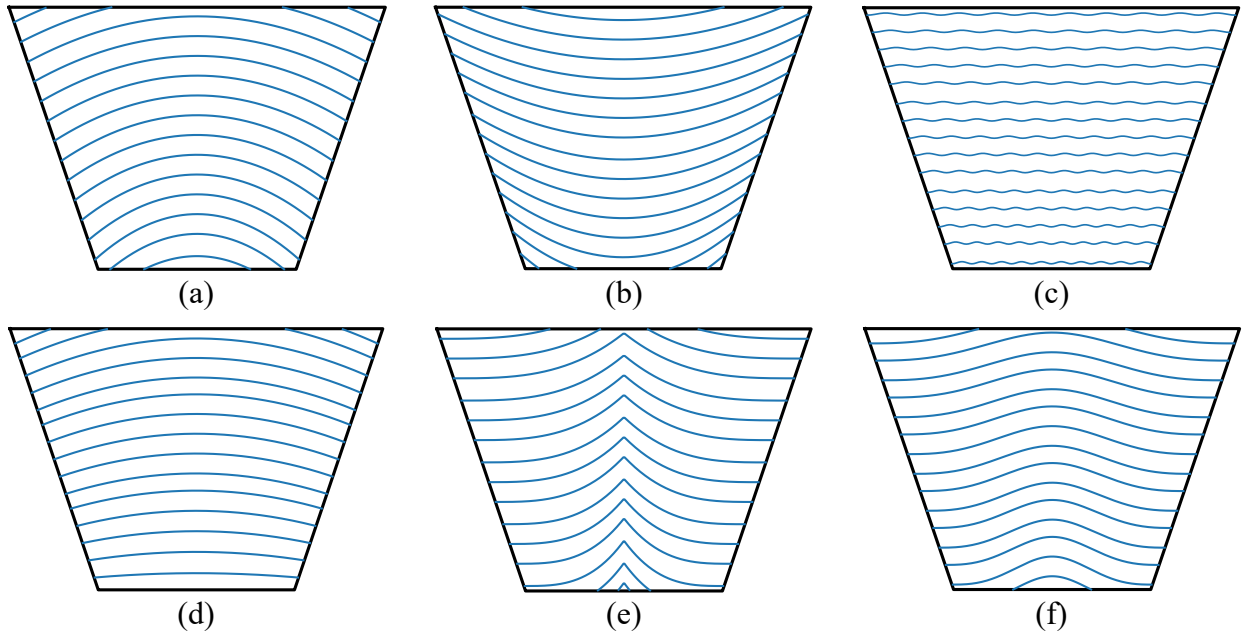

Fig. 2. Schematics of different curvilinear toolpath strategies (pyramid's side wall projection): (a) convex, (b) concave, (c) wavy, (d) adaptive, (e) cusp, and (f) sine

Different curvilinear toolpath strategies were implemented in this study, including three basic shapes proposed in previous works [14, 15] – namely convex, concave, and wavy – as well as three

newly developed variants: adaptive convex, cusp convex, and single-period sine. These variants were introduced to mitigate geometric defects observed with the basic shapes. Schematics of all toolpaths are shown in Fig. 2. The convex and concave toolpaths correspond to downward- and upward-opening parabolic profiles, respectively. For consistency and fair comparison, their amplitudes were set to the same value. The wavy toolpath is defined as a continuous sinusoidal profile with multiple periods. The adaptive convex toolpath is a modified convex profile with curvature progressively decreasing with depth. The cusp convex toolpath is defined as a convex profile with a sharp apex formed by the intersection of two parabolic segments. The single-period sine toolpath consists of one complete sinusoidal period starting and ending at valleys, with two symmetric inflection points and asymmetric convex and concave segments defined by different amplitudes or wavelengths. For consistency, the curvature of the convex segment was set to be consistent with that of the convex and concave parabolic toolpaths. A reference linear toolpath was generated in Fusion 360, from which all curvilinear toolpaths were derived. Each curvilinear strategy began and ended with several linear passes to ensure smooth transitions.

Results and Discussion

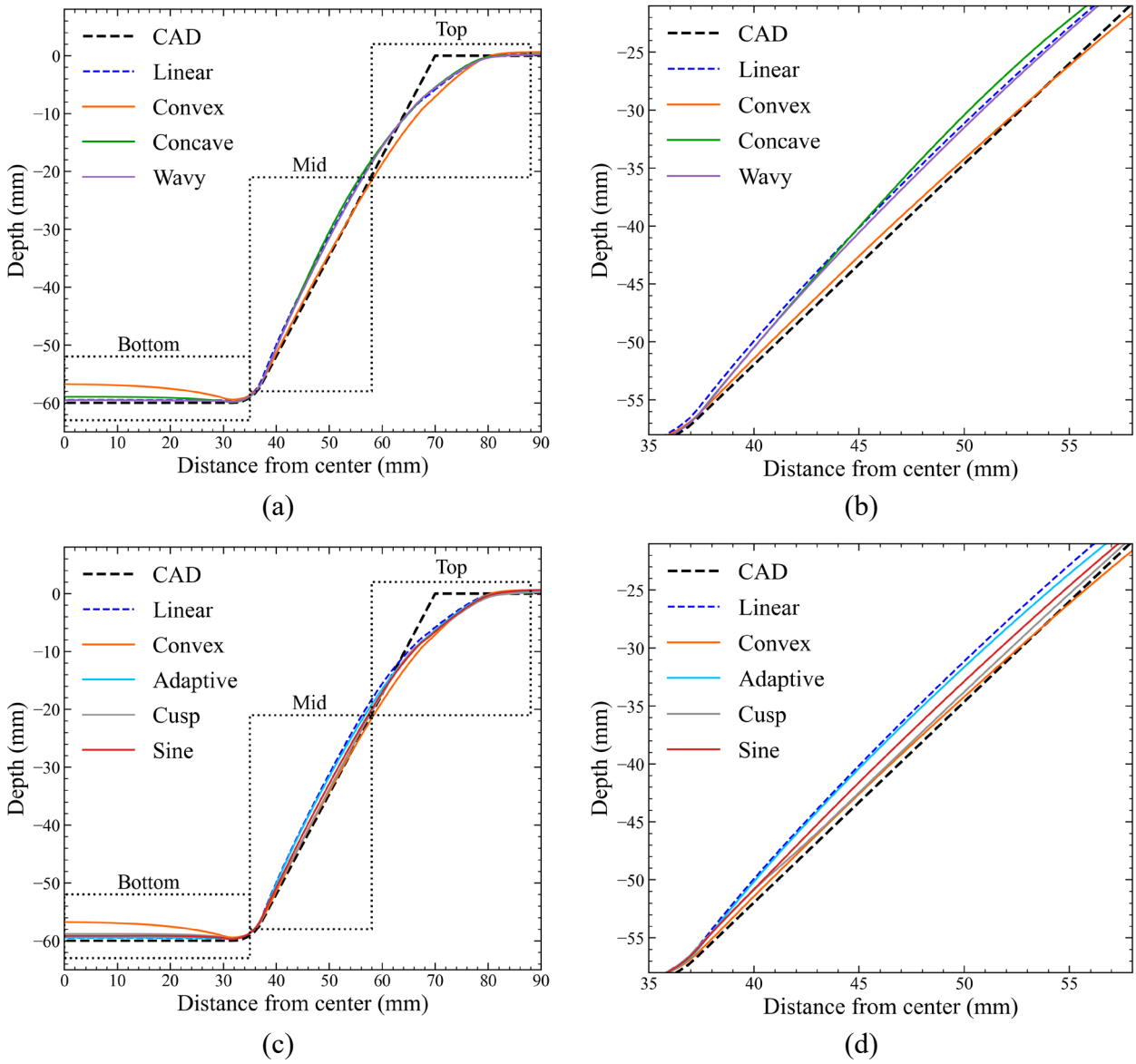

Fig. 3. Cross-sectional profile comparison of experimental results: (a) basic curvilinear toolpaths, (b) detailed view of the mid region in (a), (c) novel curvilinear toolpaths, and (d) detailed view of the mid region in (c)

Fig. 3 compares the cross-sectional profiles of experimentally formed parts produced using different curvilinear toolpaths. The profiles are divided into three regions: top, mid, and bottom. As shown in Fig. 3 (a) and Fig. 3 (c), substantial deviations from the target CAD geometry are observed in the top region for all toolpath strategies. This behavior is primarily attributed to sheet bending effects inherent to SPIF, and therefore the present analysis focuses on springback in the mid region and the pillow effect in the bottom region of the truncated pyramid. Among the basic curvilinear toolpaths (Fig. 3 (b) and Table 2), the convex toolpath exhibits the largest reduction in springback (−74.0%) relative to the conventional linear toolpath. In contrast, the concave and wavy toolpaths result in only minor changes in springback compared to the linear case, consistent with previously reported global springback trends after unclamping in open-contour parts [15]. The springback observed in the pyramid is reflected by an inward bulging of the side walls, as shown in Fig. 4, with a magnitude consistent with the springback levels observed in Fig. 3.

Table 2. Maximum springback and pillow height relative to the CAD profile

Toolpath style	Max springback [mm]	Percentage change [%]	Max pillow height [mm]	Percentage change [%]
Linear	3.651	0.0	0.509	0
Convex	0.948	-74.0	3.227	+534.1
Concave	4.270	+17.0	1.052	+106.7
Wavy	3.299	-9.6	0.468	-8.1
Adaptive	3.168	-13.2	0.562	+10.4
Cusp	1.089	-70.2	1.193	+134.4
Sine	2.147	-41.2	0.866	+70.1

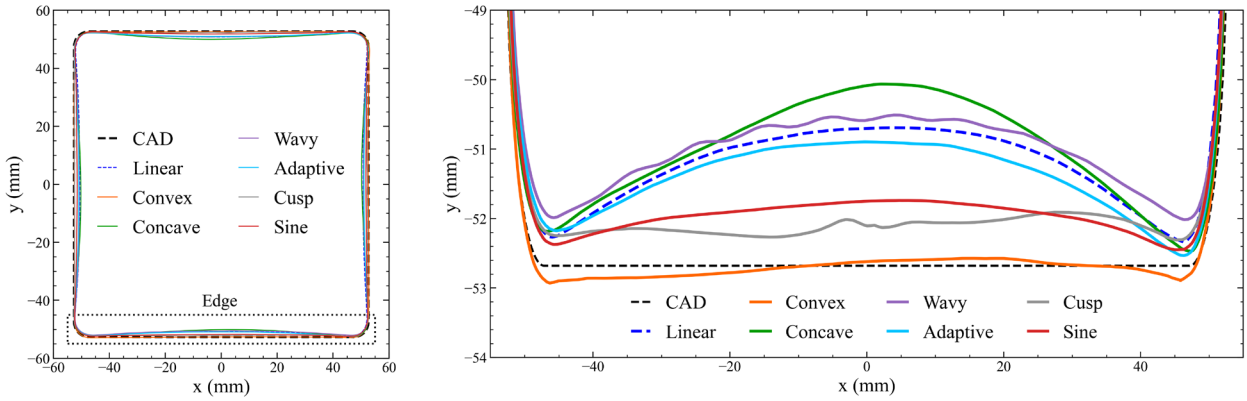

Fig. 4. Horizontal cross-sectional profile (z=-30 mm) comparison of experimental results: (a) full view, (b) detailed view of selected edge section in (a)

Despite its effectiveness in reducing springback, the convex toolpath introduces a substantially more pronounced pillow effect and reduced formability. Specifically, the convex toolpath results in a 534.1% increase in pillow height, and fracture occurred at a forming depth of approximately 70 mm during the 80 mm-deep pyramid tests, as shown in Fig. 5 (b). To mitigate these issues while maintaining low springback, three convex-inspired toolpath strategies – adaptive cusp, and sine – were proposed and evaluated, with results presented in Fig. 3 (c) and (d), Fig. 4, and Table 2. Although the adaptive toolpath effectively reduces the pillow effect, it largely restores the springback level to that of the linear toolpath, rendering it redundant compared to the baseline case. The cusp toolpath achieves substantial reductions in both springback (−70.2%) and pillow height (+134.4%); however,

it introduces a surface finish defect, as shown in Fig. 5 (a), characterized by localized thickening at the midsection of each side wall due to inhomogeneous material flow caused by the sharp change in toolpath slope at the cusp apex. The sine toolpath also provides notable reductions in springback (−41.2%) and pillow height (+70.1%) and, although slightly less effective than the cusp toolpath, produces a smoother surface without introducing additional surface finish defects. Therefore, the sine toolpath is identified as the most balanced curvilinear strategy, offering an effective compromise between springback reduction, pillow mitigation, and surface finish.

(a) (b) (c)

Fig. 5. Pyramidal parts formed using different curvilinear toolpaths: (a) cusp, (b) convex (80 mm depth), and (c) sine (80 mm depth)

To further assess the formability of the sine toolpath, an 80 mm-deep pyramid was formed using this strategy, whereas the convex toolpath failed due to severe thinning and fracture during forming. As shown in Fig. 5 (c), the pyramid was successfully formed to the full 80 mm depth without fracture, demonstrating improved formability relative to the convex toolpath. Furthermore, as shown in Fig. 6, during the forming of the 80 mm-deep pyramid, the sine toolpath achieves an overall springback reduction exceeding 50% and exhibits a negligible pillow effect compared to the linear toolpath.

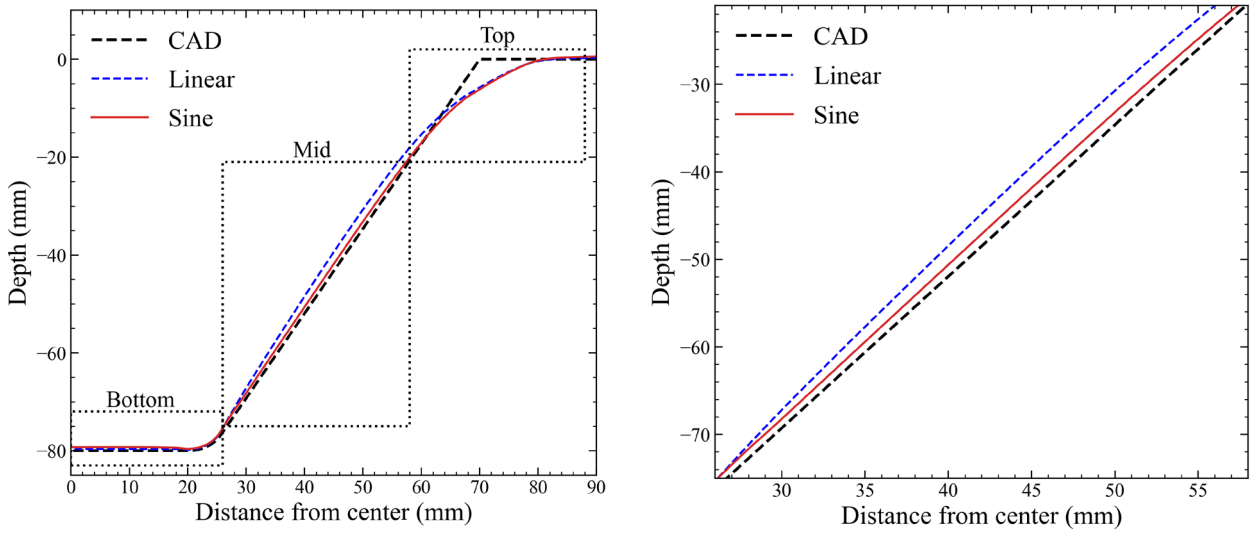

(a) (b)

Fig. 6. Cross-sectional profile comparison of experimental results of 80 mm-depth: (a) full view, and (b) detailed view of mid region in (a)

The simulated snapshots of bending moment distribution about the y-axis, SM_{22}, during forming are shown in Fig. 7. For the linear toolpath (Fig. 7 (a)), each parallel pass of the tool in the x direction leaves a positive residual bending moment (positive curvature) along the tool track. These moments accumulate along the side walls (blue circle), leading to a pronounced bulge springback, consistent

with the geometric deviations observed in Fig. 3 and 4. Although previous work [15] reported that convex toolpaths significantly reduce overall bending moments for open-contour parts prior to unclamping, Fig. 7 (b) shows that, for the closed-contour pyramid studied here, the residual bending moment along the toolpath is not markedly reduced compared to the linear case. Instead, a substantial positive residual bending moment develops in the bottom pillow region, which acts against the side walls and enhances bending near the forming edges (black circle), thereby mitigating sidewall bulging. In contrast, the concave toolpath (Fig. 7 (c)) generates negative residual bending moments in the pillow region, which do not promote edge bending (black circle) and therefore offer limited springback reduction. As shown in Fig. 7 (d), the sine toolpath produces a smaller pillow region and lower residual bending moments than the convex toolpath, which in turn leads to a moderate reduction in edge bending (black circle). Despite this reduction, the induced bending remains substantially higher than in the linear and concave cases, resulting in effective springback mitigation.

These results highlight a fundamental tradeoff between sidewall springback reduction and pillow height in closed-contour forming. Curvilinear toolpaths that induce larger positive bending moments in the pillow region tend to provide more effective springback mitigation, but excessive pillow formation can adversely affect formability. Consequently, toolpath design must balance springback control and pillow suppression based on product-specific tolerance requirements. Within this study, the sine toolpath offers the most favorable compromise, achieving substantial springback reduction while limiting pillow height and preserving formability.

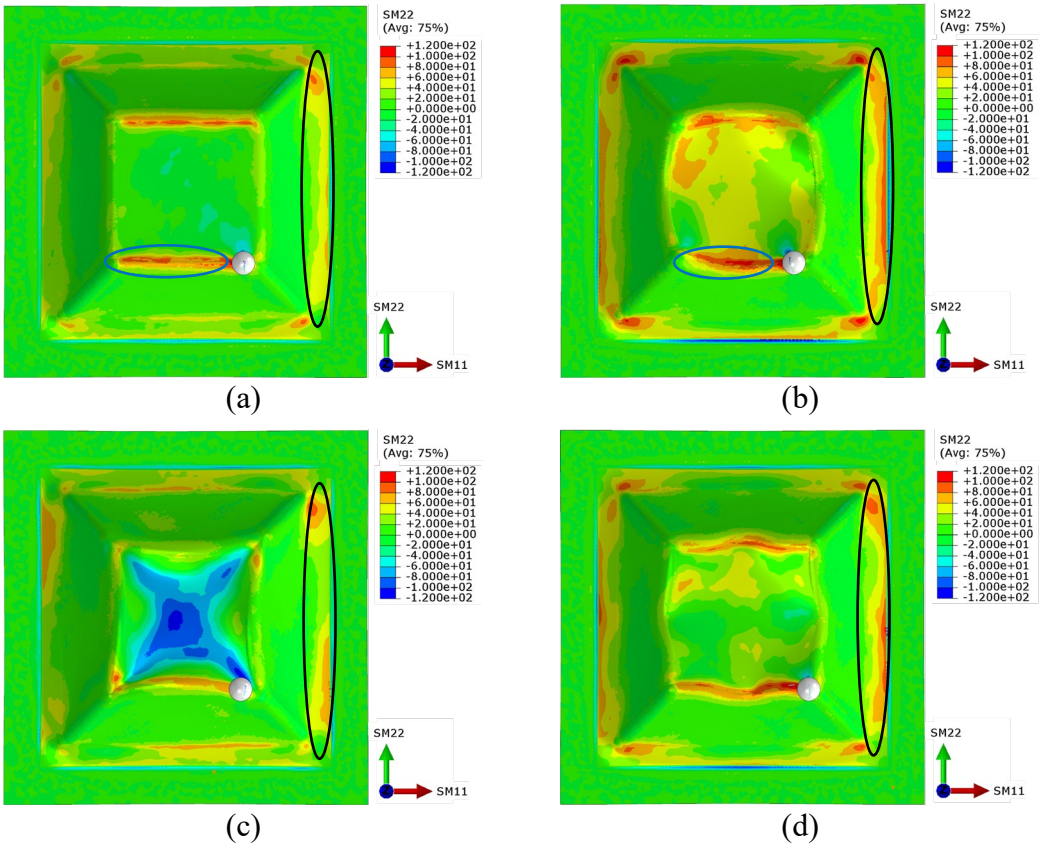

Fig. 7. Bending moment distribution for different styles of toolpaths: (a) linear, (b) convex, (c) concave, and (d) sine

Conclusion

In this study, multiple curvilinear toolpath strategies were applied to a closed-contour part using SPIF to evaluate their effectiveness in mitigating geometric defects. Three established toolpaths – convex, concave, and wavy – were examined alongside three novel toolpaths proposed in this work: adaptive, cusp, and sine. Among these, the convex toolpath achieved the greatest springback reduction in the mid-wall region; however, this benefit came at the expense of a pronounced pillow

effect and reduced formability. The cusp toolpath effectively reduced both springback and pillow height but introduced surface finish defects. Overall, the sine toolpath provided the most balanced performance, achieving effective mitigation of springback while limiting pillow formation and maintaining good formability. Deformation analysis revealed that positive sectional bending moments accumulated along the toolpath are responsible for inward bulging springback on the side walls, while positive residual bending moments in the pillow region play a critical role in springback reduction. These findings highlight an inherent tradeoff between springback mitigation and pillow severity in closed-contour part forming.

Future work may focus on the parametric optimization of curvilinear toolpath geometries to establish quantitative relationships between key mathematical features, such as amplitude and curvature, and geometric accuracy. More detailed deformation analyses could also be performed to identify the dominant deformation mechanisms associated with each toolpath type and to clarify the evolution and accumulation of residual bending moments throughout the formed part. In addition, the application of curvilinear toolpaths to closed-contour parts with curved internal wall surfaces could be investigated to assess their effectiveness in mitigating geometric defects.

References

[1] Lu, H., Liu, H. and Wang, C., 2019. Review on strategies for geometric accuracy improvement in incremental sheet forming. The International Journal of Advanced Manufacturing Technology, 102(9), pp.3381-3417.

[2] Vanhulst, M. et al., 2025. ESAFORM benchmark 2024: study on the geometric accuracy of a complex shape with single point incremental forming. International Journal of Material Forming, 18(3), p.72.

[3] Lee, Y., Mu, Z., Bansal, A., Taub, A. and Banu, M., Enhancing accuracy in two-point incremental sheet forming (TPIF): The influence of compliance and effective squeeze factor. Materials Research Proceedings, 54.

[4] Bharti, S., Paul, E., Uthaman, A., Krishnaswamy, H., Klimchik, A. and Abraham Boby, R., 2024. Systematic analysis of geometric inaccuracy and its contributing factors in roboforming. Scientific Reports, 14(1), p.20291.

[5] Behera, A.K., Verbert, J., Lauwers, B. and Duflou, J.R., 2013. Tool path compensation strategies for single point incremental sheet forming using multivariate adaptive regression splines. Computer-Aided Design, 45(3), pp.575-590.

[6] Ren, H., Xie, J., Liao, S., Leem, D., Ehmann, K. and Cao, J., 2019. In-situ springback compensation in incremental sheet forming. CIRP Annals, 68(1), pp.317-320.

[7] Bingqian, Y., Zeng, Y., Yang, H., Oscoz, M.P., Ortiz, M., Coenen, F. and Nguyen, A., 2024. Springback prediction using point series and deep learning. The International Journal of Advanced Manufacturing Technology, 132(9), pp.4723-4735.

[8] Lu, B., Chen, J., Ou, H. and Cao, J., 2013. Feature-based tool path generation approach for incremental sheet forming process. Journal of Materials Processing Technology, 213(7), pp.1221-1233.

[9] Cappellini, C., D'Urso, G. and Giardini, C., 2025. Multi-Step Tool Paths Development for Reducing Geometric Deviation and Pillow Effect in the Single-Point Incremental Forming. Journal of Manufacturing Science and Engineering, 147(7), p.071005.

[10] Vanhulst, M., Vanhove, H., Duflou, J.R., Araujo, A.C., Cantarel, A., Chabert, F., Korycki, A., Olivier, P. and Schmidt, F., 2024. Influence of toolpath strategies on the final accuracy and thickness distributions in multi-stage incremental forming. MATERIAL FORMING, ESAFORM 2024, 41, pp.1498-1506.

[11] Said, L.B., Mars, J., Wali, M. and Dammak, F., 2016. Effects of the tool path strategies on incremental sheet metal forming process. Mechanics & Industry, 17(4), p.411.

[12] Grimm, T.J. and Mears, L., 2020. Investigation of a radial toolpath in single point incremental forming. Procedia Manufacturing, 48, pp.215-222.

[13] Chang, Z., Huang, W. and Chen, J., 2020. A new tool path with point contact and its effect on incremental sheet forming process. The International Journal of Advanced Manufacturing Technology, 110(5), pp.1515-1525.

[14] Grimm, T.J., Ragai, I. and Roth, J.T., 2018. Utilization of wavy toolpath in single-point incremental forming. In ASME International Mechanical Engineering Congress and Exposition (Vol. 52019, p. V002T02A029). American Society of Mechanical Engineers.

[15] Bremen, T. and Bailly, D.B., 2024. On the Influence of Wave-Shaped Tool Path Strategies on Geometric Accuracy in Incremental Sheet Forming. Journal of Manufacturing and Materials Processing, 8(1), p.27.

[16] Shin, J., 2021. Investigation of Incremental Sheet Forming (ISF) using Advanced Numerical and Analytical Approaches. PhD thesis, University of Michigan.

[17] Burchitz, I.A., 2008. Improvement of springback prediction in sheet metal forming. PhD thesis, University of Twente.